


Review

Spinel in Meteorites: Observation Using Mössbauer Spectroscopy

Alevtina A. Maksimova ¹, Andrey V. Chukin ¹, Israel Felner ² and Michael I. Oshtrakh ^{1,*} 

¹ Department of Experimental Physics, Institute of Physics and Technology, Ural Federal University, Ekaterinburg 620002, Russia; alia55@bk.ru (A.A.M.); achukin@e1.ru (A.V.C.)

² Racah Institute of Physics, The Hebrew University, Jerusalem 91904, Israel; israel.felner@mail.huji.ac.il

* Correspondence: oshtrakh@gmail.com; Tel.: +7-912-283-7337

Received: 5 September 2018; Accepted: 9 January 2019; Published: 13 January 2019



Abstract: In this mini-review, we consider the results of various meteorite studies using Mössbauer spectroscopy with a high velocity resolution in order to reveal the minor spectral components related to spinels such as chromite, hercynite, magnesiochromite, magnesioferrite and daubréelite in bulk meteorite matter or in some extracted phases. Spinel observation in the Mössbauer spectra is supported by characterization of the studied samples by means of optical and scanning electron microscopy, energy dispersive spectroscopy, X-ray diffraction and magnetization measurements. Mössbauer parameters obtained for extraterrestrial spinels are compared with those obtained for terrestrial analogs published in the literature.

Keywords: Spinel; Meteorites; Mössbauer spectroscopy

1. Introduction

Meteorites are space messengers reaching the Earth and bringing information about solar system formation. These rocks are the result of their parent bodies' (asteroids and planets) collisions in space. A simple classification of meteorites permits us to consider three groups: stony, stony-iron and iron meteorites (more detailed meteorite classification can be found in [1] and references therein). The basic information about chemical and mineral composition of various meteorites can be found in reviews [2,3]. Almost all meteoritic minerals can be found on Earth. However, terrestrial minerals were formed in significantly different conditions in comparison with extraterrestrial minerals, which were affected by various extreme factors in space (very slow cooling, reheating, impact melting, etc.). Therefore, the phase composition of meteorites and the physical properties of their minerals are of interest for a complex investigation. All meteorites consist of iron-bearing minerals represented by Fe-Ni-Co alloy in the forms of α -Fe(Ni, Co), α_2 -Fe(Ni, Co), γ -Fe(Ni, Co) and γ -FeNi phases, olivine (Fe, Mg)₂SiO₄, orthopyroxene (Fe, Mg)SiO₃, clinopyroxene (Fe, Mg, Ca)SiO₃, troilite FeS and some other minerals. Iron-bearing spinels can also be found in meteorites as the minor accessory minerals. Some of them, for example daubréelite (FeCr₂S₄) and chromite (FeCr₂O₄), were formed with meteorite matter in space. Other spinels such as magnetite (Fe₃O₄) or magnesioferrite (MgFe₂O₄) can be a result of meteorites weathering (oxidation) in the terrestrial conditions. Since all these minerals contain iron, it is possible to use ⁵⁷Fe Mössbauer spectroscopy for studying meteorites. About 55 years of experience demonstrate significant progress in the development of Mössbauer spectroscopy of various meteorites from the first review [4] until the modern studies (see, for instance, [5,6]). However, the Mössbauer spectra of meteorites are very complex and consist of various numbers of major and minor components related to different phases and mineral compositions of rocks. Therefore, revealing of the minor phases, for instance, spinels, appears to be very difficult in the Mössbauer spectra of bulk meteorite samples. Therefore, we used Mössbauer spectrometers with a high velocity

resolution. The velocity driving system in these spectrometers has the higher discretization of the velocity reference signal (2^{12} versus 2^9 in conventional spectrometers). This leads to the smaller Doppler modulation step for resonant γ -quanta energy, that is why the high velocity resolution Mössbauer spectroscopy is a useful technique for excavating the minor components in the complex spectra due to much higher sensitivity, precision and accuracy than those in conventional Mössbauer spectrometers. Some advances of this method in meteorites study have been considered in [7–9]. Therefore, in this mini-review, we consider our results related to the observation of various spinel phases in meteorites using the high velocity resolution Mössbauer spectroscopy. Additional information obtained by other techniques such as optical microscopy, scanning electron microscopy (SEM) with energy dispersive spectroscopy (EDS), X-ray diffraction (XRD) and magnetization measurements is used for supporting observation of spinels.

2. Materials and Methods

We studied several fragments of different ordinary chondrites (Chelyabinsk LL5 No 1a and No 2, Northwest Africa (NWA) 6286 LL6 and NWA 7857 LL6, Tsarev L5 and Annama H5), Seymchan main group pallasite (PMG) and troilite inclusion extracted from Sikhote-Alin IIAB iron meteorite. Polished sections of these meteorite fragments were prepared by the standard method for samples characterization by optical microscopy and SEM with EDS. Powdered samples were then prepared from the polished surfaces for XRD, magnetization measurements and Mössbauer spectroscopy. Additionally, the fusion crust from Chelyabinsk LL5 fragment No 1a and the massive troilite inclusion from the Sikhote-Alin iron meteorite were removed and prepared as a powder for the study. Details of different samples preparation and characterization were described in [9–15].

Meteorites characterization was done using an Axiovert 40 MAT optical microscope (Carl Zeiss, Oberkochen, Germany), a SIGMA VP electron microscope (Carl Zeiss, Oberkochen, Germany) with an X-max 80 (Oxford Instruments, Abingdon, Oxfordshire, England) energy dispersive spectroscopy device, an AMRAY 1830 scanning electron microscope equipped with EDAX PV9800 energy dispersive spectrometer, X-ray diffractometers Shimadzu XRD-7000 and Panalytical X'Pert Pro MPD and commercial SQUID magnetometer MPMS-5S (Quantum Design, San Diego, CA, USA).

Mössbauer spectra were measured using an automated precision Mössbauer spectrometric system built on the base of the SM-2201 spectrometer with a saw-tooth shape velocity reference signal formed by the digital-analog converter using discretization of 2^{12} (quantification of the velocity reference signal using 4096 steps) and a liquid nitrogen cryostat with moving absorber. The high level of the velocity scale discretization provides much better adjustment to resonance, and significantly increases the spectra quality and analytical possibilities of Mössbauer spectroscopy. On the other hand, this increases the measurement time. Registration of γ -rays was done using scintillator detector with NaI(Tl) crystal with a thickness of 0.1 mm. Details and characteristics of this spectrometer and the system as well as this method's features are described in [16,17]. The $(1.8\text{--}1.0) \times 10^9$ Bq ^{57}Co in rhodium matrix sources (Ritverc GmbH, St. Petersburg, Russian Federation) were at room temperature. The Mössbauer spectra were measured in transmission geometry with moving absorber in the cryostat and recorded in 4096 channels. To increase the signal-to-noise ratio in the complex spectra with the minor components, they were converted into 1024 channels by consequent summation of four neighboring channels to reach higher statistics and larger signal-to-noise ratio (details for each sample study are given in [9–15]).

Mössbauer spectra were computer-fitted with a UNIVEM-MS program using the least squares procedure with a Lorentzian line shape. This procedure uses the usual perturbation of the first order method for magnetically split components. Therefore, the spectral component of troilite, which requires the full static Hamiltonian for the fit, cannot be fitted correctly. To overcome this problem, the Mössbauer spectra containing troilite component were fitted using a simulation of the full static Hamiltonian by means of the method described in detail in [18,19]. The results obtained are very close to parameters for the minor spectral components obtained from the ordinary chondrites Mössbauer spectra fits using both the full static Hamiltonian and above-mentioned simulation method.

The spectral parameters, such as isomer shift, δ , quadrupole splitting, ΔE_Q , quadrupole shift for magnetically split spectra, ε ($\Delta E_Q = 2\varepsilon$), hyperfine magnetic field, H_{eff} , line width (a full width at a half maximum), Γ , relative subspectrum area, A , and statistical quality of the fit, χ^2 , were determined. Calibration of the velocity scale was made using the reference absorber of α -Fe foil with a thickness of 7 μm . The line shapes were pure Lorentzian with the first and the sixth, the second and the fifth, and the third and the fourth line widths values of $\Gamma_{1,6} = 0.238 \pm 0.008$ mm/s, $\Gamma_{2,5} = 0.232 \pm 0.008$ mm/s and $\Gamma_{3,4} = 0.223 \pm 0.008$ mm/s for the α -Fe spectrum recorded in 4096 channels. The velocity range was about $\pm(10-7)$ mm/s depending on the studied sample. The instrumental (systematic) error for each spectrum point was ± 0.5 channel (the velocity scale). The instrumental (systematic) error for the hyperfine parameters was ± 1 channel. If an error calculated with the fitting procedure (fitting error) for these parameters exceeded the instrumental (systematic) error, we used the larger error instead. Relative error for A did not usually exceed 10%. Criteria for the best fits were differential spectrum, χ^2 and physical meaning of the spectral parameters. Isomer shifts are given relative to α -Fe at 295 K.

To demonstrate the difference in the quality of the Mössbauer spectra measured with conventional velocity resolution and with a high velocity resolution, we show a comparison of the Mössbauer spectra of Mount Tazerzait L5 ordinary chondrite samples in Figure 1. This comparison could be good evidence of the effect of increasing the velocity resolution (discretization of the velocity reference signal) in Mössbauer spectrometers and spectra.

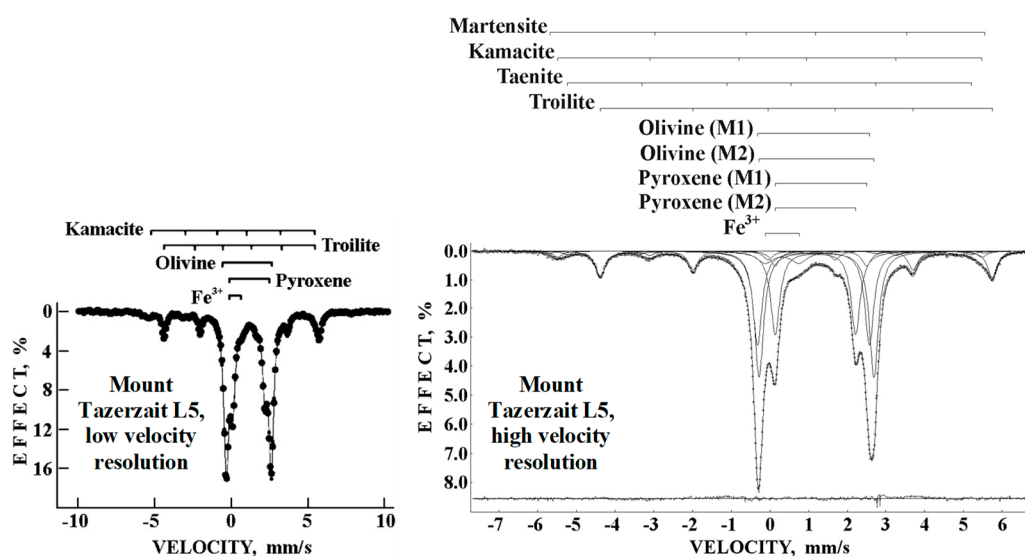


Figure 1. Mössbauer spectra of Mount Tazerzait L5 samples measured: (left) using conventional Mössbauer spectrometer with a low velocity resolution and folding (in 256 channels) from Ref. [8] cited in [17]; and (right) using Mössbauer spectrometer SM-2201 with a high velocity resolution (4096 channels) without folding (this spectrum was further converted into 1024-channel spectrum to increase signal-to-noise ratio for the minor spectral components); the differential spectrum is shown below. $T = 295$ K. Adopted from [17].

3. Results and Discussion

Spinel phases were observed in all studied samples. However, these spinels were different for different types of meteorites. Therefore, we consider these results for stony (ordinary chondrites), stony-iron (main group pallasite) and iron meteorites separately.

3.1. Chromite in Ordinary Chondrites

Optical microscopy of polished sections of Chelyabinsk LL5, NWA 6286 LL6, NWA 7857 LL6, Tsarev L5 and Annama H5 fragments demonstrated the presence of silicate phases with small metallic Fe-Ni-Co grains, troilite and chromite inclusions. A representative optical microphotograph of the

NWA 6286 polished section is shown in Figure 2a. SEM with EDS demonstrated the presence of olivine, pyroxenes, troilite, α -Fe(Ni, Co) and γ -Fe(Ni, Co) phases and chromite (representative SEM image of NWA 6286 is shown in Figure 2b).

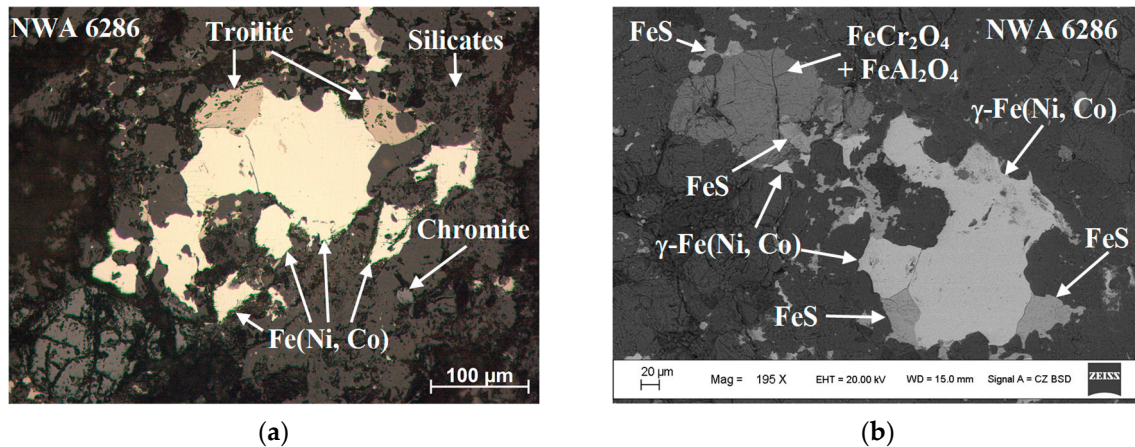


Figure 2. Microphotographs of NWA 6286 polished section obtained using: (a) optical microscopy; and (b) scanning electron microscopy. Adopted from [13].

Chemical analysis of selected chromite inclusions in Chelyabinsk LL5, NWA 6286 LL6, NWA 7857 LL6, Tsarev L5 and Annama H5 fragments carried out with EDS showed some variations in metal content (see Table 1). These inclusions contain Cr and Fe as the main metals. However, it was found the presence of Al as the third metal, except chromite in Tsarev L5. In chromite inclusions of the latter ordinary chondrite Mg and Al were presented with a similar content as the third and the fourth metals. The presence of Al as the third metal in chromite inclusions indicates the formation of additional spinels such as hercynite FeAl₂O₄ or mixed Fe(Al_{1-x}Cr_x)₂O₄ spinel. Therefore, XRD patterns of Chelyabinsk LL5, NWA 6286 LL6, NWA 7857 LL6, Tsarev L5 and Annama H5 fragments were fitted using the Rietveld full profile analysis without and with accounting for the minor spinel phases of chromite and hercynite. A comparison of both fits demonstrated that accounting for two minor spinels led to a better fitting quality (representative XRD pattern for the powdered bulk NWA 6286 matter is shown in Figure 3a). The phase composition for studied meteorites is presented in Table 2. It should be noted that the presence of Mg in chromite in Tsarev L5 is comparable with Al content and therefore indicates the presence of Mg-bearing spinels. We have so far been unable to reveal these minor spinels from this XRD pattern. However, measurements of the zero-field-cooled (ZFC) and field-cooled (FC) magnetization curves for NWA 6286 LL6, NWA 7857 LL6, Tsarev L5 and Annama H5 fragments demonstrated the phase transition in the temperature range of 48–60 K (see representative ZFC/FC curves in Figure 3b for NWA 6286). This temperature range is in agreement with the range for Curie temperature of 40–80 K for the chromite ferrimagnetic-paramagnetic phase transition in various ordinary chondrites obtained in [20].

Table 1. Average values and ranges of the content (in at. %) of some metals determined in selected chromite inclusions in ordinary chondrites by energy dispersive spectroscopy.

Metal	Chelyabinsk LL5 No 1a	Chelyabinsk LL5 No 2	NWA 6286 LL6	NWA 7857 LL6	Tsarev L5	Annama H5
Fe	13.2	13.1	12.2–13.5	10.2–16.1	10.7	8.0–8.4
Cr	21.2	21.0	19.9–21.6	17.5–28.4	21.1	15.2–16.1
Al	3.5	3.9	3.1–3.8	3.3–4.8	3.2	2.8–3.0
Mg	1.5	1.3	1.5–1.9	1.2–2.0	3.7	1.8–1.4
Ti	1.0	0.6	0.9–1.6	0.2–1.1	1.0	0.4

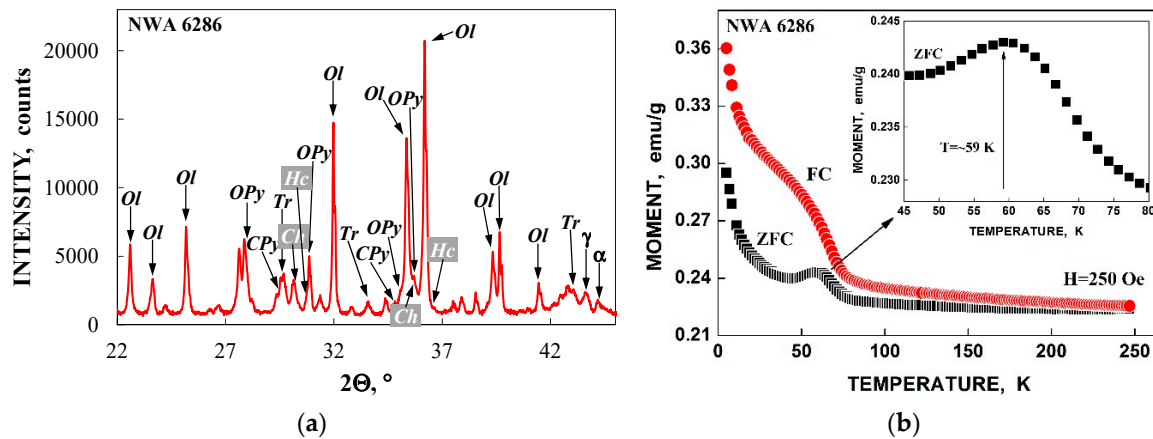


Figure 3. Characterization of the powdered bulk NWA 6286 matter: (a) X-ray diffraction pattern with indication of some reflexes of the iron-bearing phases: Ol is olivine, OPy is orthopyroxene, CPy is clinopyroxene, Tr is troilite, Ch is chromite, Hc is hercynite, α is α -phase, and γ is γ -phase. (b) Zero-field-cooled (ZFC) and field-cooled (FC) magnetization curves with inset that shows an enlarged part of ZFC curve indicated the phase transition in chromite. Adopted from [13].

Table 2. Phase composition (in wt.%) of some ordinary chondrites determined by X-ray diffraction.

Phase/Mineral	Chelyabinsk LL5 No 1a ¹	Chelyabinsk LL5 No 2 ²	NWA 6286 LL6 ³	NWA 7857 LL6 ³	Tsarev L5 ⁴	Annama H5 ⁵
Olivine	50.6	48.6	57.3	59.2	43.1	38.6
Anorthite	8.2	8.2	11.8	9.4	9.7	4.7
Orthopyroxene	31.9	25.2	18.9	19.9	28.6	36.6
Clinopyroxene	5.5	6.9	3.7	3.6	6.2	1.4
Troilite	6.7	6.2	4.8	3.6	7.2	5.6
α -Fe(Ni, Co)	1.4	1.8	0.2	1.8		9.0
γ -Fe(Ni, Co)	0.9	0.8	1.2	0.5	0.6	1.3
Chromite	1.5	1.5	1.7	1.7	3.5	2.7
Hercynite	0.4	0.8	0.4	0.3	0.7	0.2

¹ [9]; ² submitted for publication; ³ [13]; ⁴ [14]; ⁵ [12].

Two representative Mössbauer spectra of non-weathered LL ordinary chondrites are shown in Figure 4.

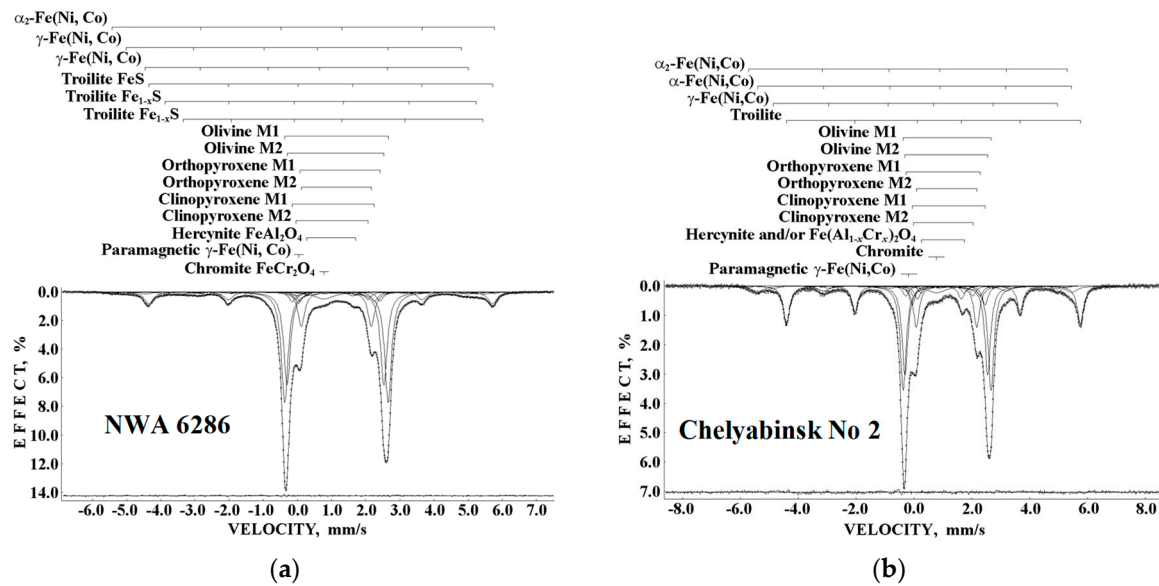


Figure 4. Mössbauer spectra of LL ordinary chondrites: (a) NWA 6286; and (b) Chelyabinsk, fragment No 2. Indicated components are the results of the best fits. The differential spectra are shown below. $T = 295$ K. Adopted from [13,21], respectively.

These spectra demonstrate a very complex composition of different magnetic and paramagnetic components. The best fits of the Chelyabinsk LL5 (fragments No 1a and No 2), NWA 6286 LL6 and NWA 7857 LL6 Mössbauer spectra revealed components which were related to the M1 and M2 sites in silicate phases (olivine, orthopyroxene and clinopyroxene), ferromagnetic α_2 -Fe(Ni, Co), α -Fe(Ni, Co) and γ -Fe(Ni, Co) phases and a paramagnetic γ -Fe(Ni, Co) phase, troilite and non-stoichiometric troilite Fe_{1-x}S , chromite and hercynite and/or mixed $\text{Fe}(\text{Al}_{1-x}\text{Cr}_x)_2\text{O}_4$ spinel on the basis of Mössbauer hyperfine parameters. It is well known that the Mössbauer spectra of normal chromites measured at room temperature demonstrate single-peak shapes, which were fitted as a quadrupole doublet with a very small value of quadrupole splitting: $\Delta E_Q = 0.15$ mm/s in [22] and $\Delta E_Q = 0.06$ mm/s ($\delta = 0.92$ mm/s) in [23], or as a single line with $\delta = 0.90$ mm/s in [24], $\delta = 0.92$ mm/s in [25] and $\delta = 0.93$ mm/s in [26]. However, experimental observation of ΔE_Q value, which is smaller than the ^{57}Fe natural line width (0.19 mm/s), is doubtful because, in fact, any Lorentzian line can be decomposed into two equal Lorentzian lines with slightly different peak positions. Therefore, it is reasonable to consider a paramagnetic single line for the chromite Mössbauer spectrum. In contrast, the Mössbauer spectra of hercynite and mixed $\text{Fe}(\text{Al}_{1-x}\text{Cr}_x)_2\text{O}_4$ spinel demonstrated a quadrupole doublet with the following hyperfine parameters: $\delta = 0.91$ mm/s and $\Delta E_Q = 1.57$ mm/s obtained for hercynite in [24], while ΔE_Q value for the mixed $\text{Fe}(\text{Al}_{1-x}\text{Cr}_x)_2\text{O}_4$ spinel may vary depending on x (see [27]). Suggesting small x values, we can consider similar Mössbauer hyperfine parameters for these spinels and use one quadrupole doublet to fit component assigned to hercynite and/or mixed $\text{Fe}(\text{Al}_{1-x}\text{Cr}_x)_2\text{O}_4$ spinel.

Revealing the chromite component in the Mössbauer spectra of weathered ordinary chondrites is very complex because the spectral component related to the paramagnetic ferric compounds overlaps with chromite single peak (see [19,21]). Nevertheless, measurement of the Mössbauer spectrum of the weathered Tsarev L5 new fragment with better quality than in a previous study [19] permitted us to reveal spectral components associated with chromite and hercynite (Figure 5a). However, it was not possible to find spectral components related to Mg-bearing spinels. The latter spinels can be presented at least by magnesioferrite MgFe_2O_4 or by magnesiochromite $(\text{Fe}_{1-x}\text{Mg}_x)\text{Cr}_2\text{O}_4$. The room temperature Mössbauer spectrum of bulk magnesioferrite demonstrates magnetic ordering with two six-line patterns related to the ^{57}Fe in tetrahedral (A) and octahedral [B] positions with hyperfine parameters: $\delta_A = \sim 0.26$ mm/s, $H_{\text{eff}}^A = 464$ kOe; $\delta_B = \sim 0.35$ mm/s, $H_{\text{eff}}^B = 496$ kOe, respectively

(see, for instance, [28,29]). Therefore, it is not possible to observe a very small contribution of possible magnesioferrite magnetic sextets beyond the spectral noise. The room temperature Mössbauer spectrum of magnesiochromite is similar to chromite and demonstrates the paramagnetic singlet with δ value of about 0.9 mm/s (see [23]). In this case, it is very difficult to extract correctly a very small singlet component in addition to a singlet related to chromite with relatively larger area, when both singlets overlap with a doublet related to ferric compounds with much larger relative area. For example, when we introduced an additional small singlet line into the fitting model, we obtained slightly better fit with two singlets with the following parameters: $\delta = 0.855 \pm 0.015$ mm/s, $A \approx 1.3(1)$ % and $\delta = 1.198 \pm 0.019$ mm/s, $A \approx 0.7(1)$ %. The first singlet can be related to chromite while the second one can be assigned to magnesiochromite with a larger δ value than that obtained in [23]. However, the reliability of this result can be confirmed in the case of the study of non-weathered ordinary chondrites with similar chemical composition of chromite inclusions. As for quadrupole doublet associated with hercynite and/or mixed $\text{Fe}(\text{Al}_{1-x}\text{Cr}_x)_2\text{O}_4$ spinel, its presence can be found by analysis of the small peak at about +1.7 mm/s, which is related mainly to the fourth peak in the troilite sextet. The six-line pattern for troilite should be fitted with the constrained peak areas ratio $A_{1,6}:A_{2,5}:A_{3,4} = 3:2:1$. In the fit without a quadrupole doublet associated with hercynite and free variation of troilite sextet areas, the value of $A_{3,4}$ is larger to keep the required constraint, while the fit with this constraint shows a misfit at the differential spectrum for the peak at about ± 1.7 mm/s. Adding the quadrupole doublet, which can be related to hercynite, improves the fit, while Mössbauer parameters of this doublet are suitable to be associated with hercynite and/or mixed $\text{Fe}(\text{Al}_{1-x}\text{Cr}_x)_2\text{O}_4$ spinel. A similar approach was used for the above-mentioned non-weathered ordinary chondrites.

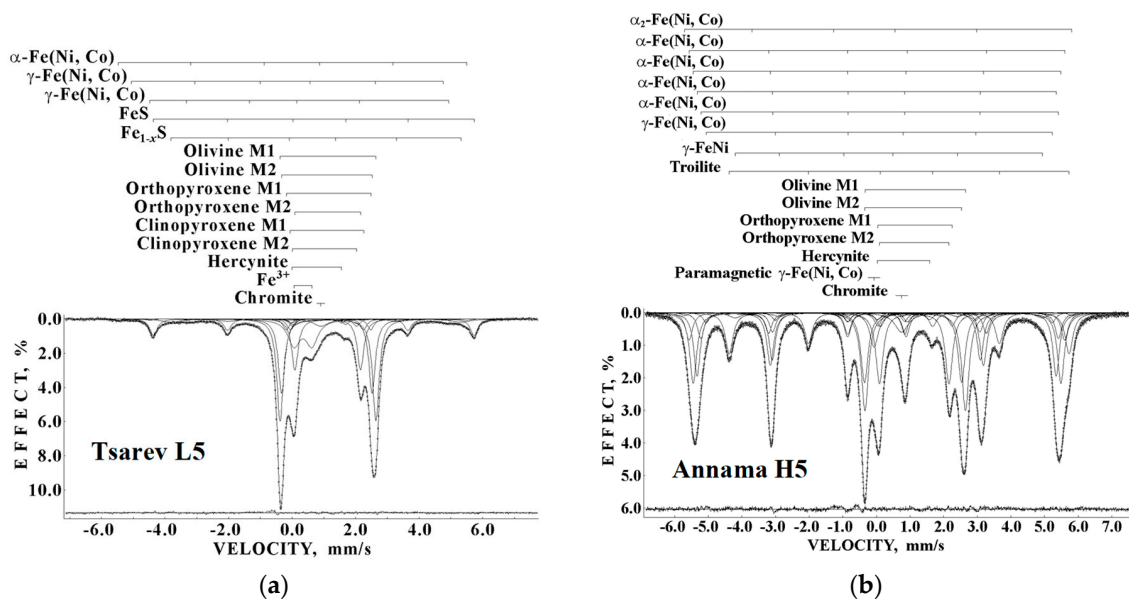


Figure 5. Mössbauer spectra of L and H ordinary chondrites: (a) Tsarev L5; and (b) Annama H5. Indicated components are the results of the best fits. The differential spectra are shown below. $T = 295$ K. Adopted from [12,14], respectively.

The Mössbauer spectrum of non-weathered Annama H5 (Figure 5b) shows a huge contribution of components related to Fe-Ni-Co alloy. In this spectrum, there is also a problem with revealing the minor components related to spinels, which overlap with other spectral components. However, in this spectrum, it was also possible to find spinel components because: (i) an envelope peak at about +0.9 mm/s demonstrates some features, which can be better fitted using a minor singlet peak in addition to the overlapped fourth peaks of seven magnetic sextets related to the Fe-Ni-Co phases; and (ii) additional quadrupole doublet is needed for the better fit of the fourth peak of troilite sextet at about +1.7 mm/s similar to those described for the Tsarev L5 Mössbauer spectrum.

Mössbauer parameters obtained for chromite and hercynite and/or mixed $\text{Fe}(\text{Al}_{1-x}\text{Cr}_x)_2\text{O}_4$ spinel from the Mössbauer spectra of ordinary chondrites are presented in Table 3 in comparison with data for synthetic chromite and hercynite.

Table 3. Mössbauer parameters for spinels found in the bulk ordinary chondrites in comparison with data obtained for synthetic spinels.

Parameter	Chelyabinsk LL5 No 1a ¹	Chelyabinsk LL5 No 2 ²	NWA 6286 LL6 ³	NWA 7857 LL6 ⁴	Tsarev L5 ³	Annama H5 ⁵	Synthetic Spinel ⁶
Chromite							
Γ , mm/s	0.776 ± 0.107	0.776 ± 0.034	0.700 ± 0.028	0.776 ± 0.028	0.568 ± 0.030	0.498 ± 0.028	0.33
δ , mm/s	0.855 ± 0.026	0.777 ± 0.017	0.776 ± 0.014	0.662 ± 0.014	0.909 ± 0.015	0.748 ± 0.014	0.90
A, %	~1.6(2)	~2.7(3)	~3.1(3)	~2.9(3)	~2.3(2)	~2.4(2)	100
Hercynite and/or mixed $\text{Fe}(\text{Al}_{1-x}\text{Cr}_x)_2\text{O}_4$ spinel							
Γ , mm/s	0.234 ± 0.033	0.238 ± 0.033	0.235 ± 0.028	0.237 ± 0.028	0.246 ± 0.030	0.260 ± 0.028	0.75
δ , mm/s	0.883 ± 0.027	0.997 ± 0.017	0.987 ± 0.014	0.959 ± 0.014	0.843 ± 0.015	0.852 ± 0.014	0.91
ΔE_Q , mm/s	1.499 ± 0.469	1.480 ± 0.017	1.434 ± 0.014	1.504 ± 0.014	1.414 ± 0.018	1.465 ± 0.014	1.57
A, %	~0.7(1)	~1.7(2)	~0.9(1)	~1.6(2)	~1.0(1)	~0.9(1)	100

¹ [9]; ² [21]; ³ [13]; ⁴ [14]; ⁵ [12]; ⁶ [24].

3.2. Chromite in Seymchan Main Group Pallasite

Characterization of the stony part of a slightly weathered Seymchan PMG fragment using optical microscopy showed the presence of olivine with inclusions of troilite and chromite (Figure 6a). SEM with EDS confirmed the presence of troilite and chromite inclusions in olivine while stony fragments were imbedded in Fe-Ni-Co alloy matrix (Figure 6b). Chemical analysis of chromite inclusions demonstrated the presence of ~26–28 at.% of Cr, ~9–10 at.% of Fe, ~5–6 at.% of Mg and ~0.7–1 at.% of Al. In contrast to chromite in the studied ordinary chondrites, chromite inclusions in the stony part of Seymchan PMG contain Mg as the third metal, while Al content is significantly smaller. Therefore, chromite inclusions can also contain Mg-bearing spinels. For example, magnesiochromite may be a result of Fe substitution by Mg. However, EDS cannot distinguish the presence of magnesiochromite or magnesioferrite in chromite.

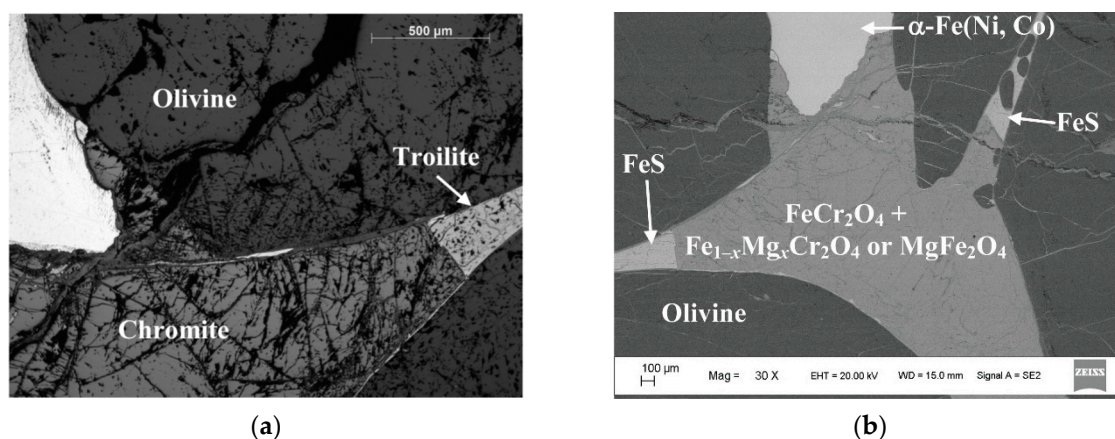


Figure 6. Characterization of the stony part of Seymchan main group pallasite: (a) optical microphotograph; and (b) scanning electron microscopy image with the results of energy dispersive spectroscopy. Adopted from [15].

The results of further characterization of the stony part extracted from Seymchan PMG by XRD and magnetization measurements are shown in Figure 7. The fit of the XRD pattern demonstrates that there are positions of minor reflexes corresponding to chromite and magnesiochromite instead of MgFe_2O_4 . The phase composition of the stony part from Seymchan PMG was determined as follows: olivine (~95.5 wt.%), clinopyroxene (~2.3 wt.%), chromite (~1.1 wt.%), troilite (~0.3 wt.%) and mixed iron-magnesium chromite (~0.8 wt.%).

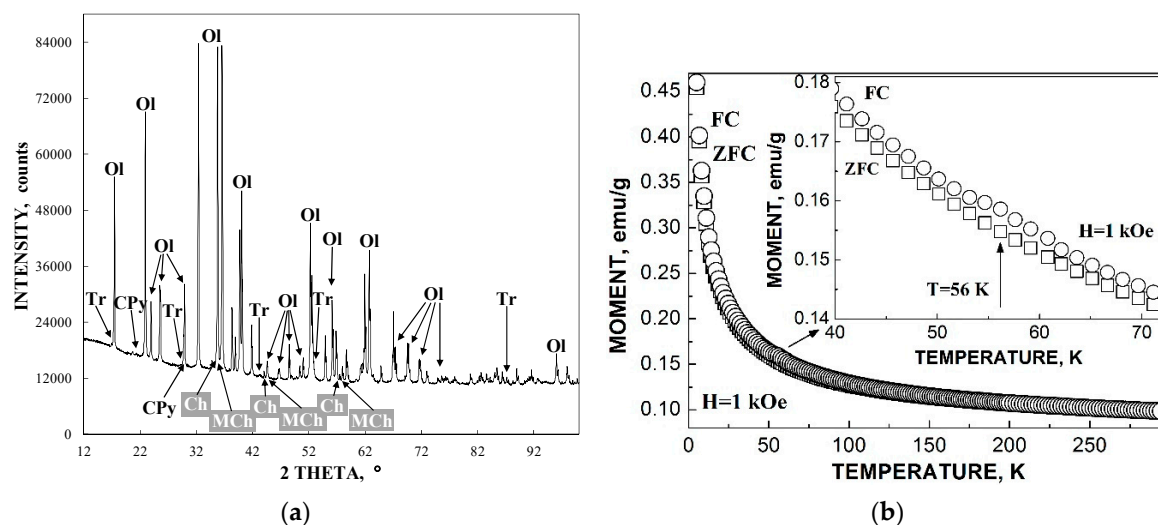


Figure 7. Stony part of Seymchan main group pallasite: (a) X-ray diffraction pattern with indication of some reflexes of the iron-bearing phases: Ol is olivine, CPy is clinopyroxene, Tr is troilite, Ch is chromite, and MCh is magnesiochromite. (b) Zero-field-cooled (ZFC) and field-cooled (FC) magnetization curves with inset which shows enlarged part of ZFC/FC curves indicated a small bulge, probably related to the phase transition in chromite. Adopted from [15].

Magnetization measurements showed a very weak bulge at 56 K, which is from the range of Curie temperature for chromite [20]. The reason for so small bulge in comparison with that for ordinary chondrites (see Figure 3b) might be explained as follows. Chromite should be randomly distributed in the bulk material, that is why very low chromite content appeared to be in the sample of few mg that was taken for magnetization measurements from the bulk powder.

The Mössbauer spectra of the stony part extracted from Seymchan PMG were measured in large and small velocity ranges (Figure 8) to check the presence of magnetically split components (troilite and magnesioferrite demonstrate magnetically split spectra at room temperature). The Mössbauer spectrum measured in a large velocity range showed only one magnetic sextet related to troilite. This spectrum was decomposed also in several quadrupole doublets related to silicate phases and unknown ferrous and ferric compounds and one singlet which was attributed to chromite. The presence of a weak ferric spectral component did not prevent us revealing a singlet subspectrum. To increase resolution in the spectrum, we measured the same sample in a small velocity range. The same spectral components were used to fit this spectrum (for troilite subspectrum, we know peak positions for the second and the fifth, and the third and the fourth lines in the sextet). However, to reach the best fit, we had to add an additional minor single line to fit the envelope spectrum feature in the range +0.5–1.2 mm/s. Mössbauer parameters for these two singlets are as follows: $\Gamma = 0.776 \pm 0.016$ mm/s, $\delta = 0.886 \pm 0.009$ mm/s, and $A = \sim 3.4(3)$ % and $\Gamma = 0.213 \pm 0.016$ mm/s, $\delta = 0.796 \pm 0.021$ mm/s, and $A = \sim 0.20(2)$ %. A singlet with relatively larger area was associated with chromite while the second singlet was assigned to magnesiochromite. The δ value for magnesiochromite determined in the stony part of Seymchan PMG is slightly smaller than the $\delta = 0.92$ mm/s value obtained for synthetic magnesiochromite samples in [23]. The δ value for chromite in the stony part extracted from Seymchan PMG is in agreement with the range of δ values shown for chromites in Table 3.

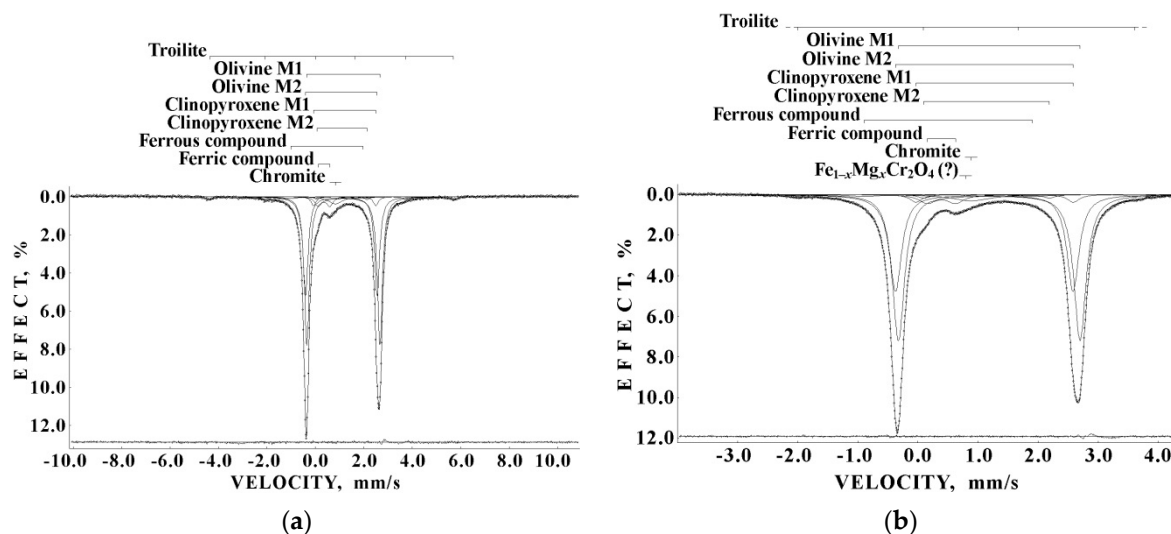


Figure 8. Mössbauer spectra of the stony part of Seymchan main group pallasite measured in: (a) large velocity range; and (b) small velocity range. Indicated components are the results of the best fits. The differential spectra are shown below. $T = 295$ K. Adopted from [15].

3.3. Daubréelite in Troilite Extracted from the Sikhote-Alin Iron Meteorite

A massive troilite inclusion was found in the polished section of one fragment of the Sikhote-Alin IIAB iron meteorite (Figure 9a). This troilite, extracted from the α -Fe(Ni, Co) matrix, was analyzed by SEM with EDS (Figure 9b). Chemical analysis of several troilite particles demonstrated the presence of ~ 34 wt.% of S, ~ 65 wt.% of Fe and ~ 1 wt.% of Cr (averaged values). The latter can indicate that there is a small amount of daubréelite FeCr_2S_4 in troilite extracted from the Sikhote-Alin iron meteorite. The XRD pattern of the troilite inclusion was measured and fitted using the full profile Rietveld analysis (Figure 10a). The results showed the presence of ~ 93 wt.% of troilite and ~ 7 wt.% of daubréelite. The unit cell of this daubréelite (cubic spinel structure, space group $Fd\bar{3}m$) with parameters $a = b = c = 9.98(5)$ Å is shown in Figure 10b.

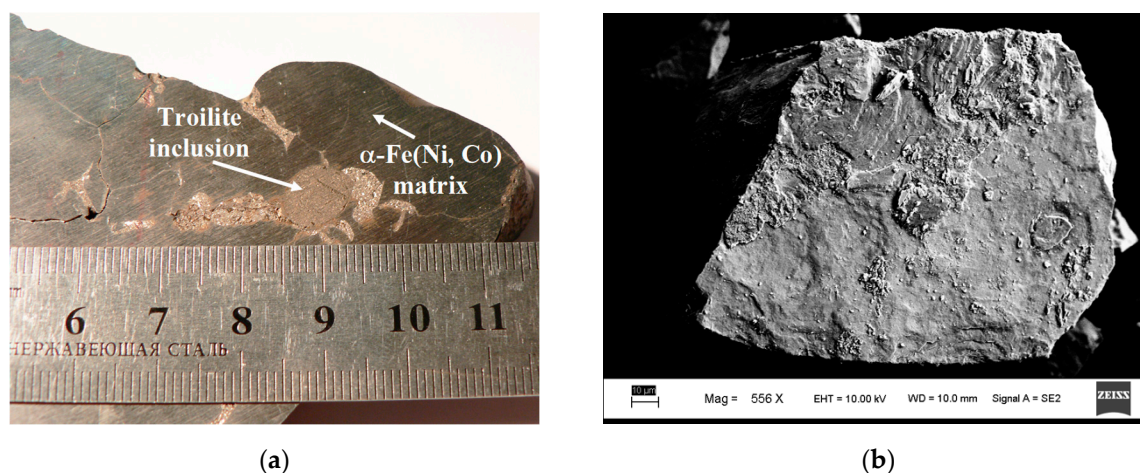


Figure 9. Troilite inclusion in Sikhote-Alin IIAB iron meteorite: (a) photograph of massive troilite inclusion in α -Fe(Ni, Co) matrix; and (b) scanning electron microscopy image of troilite particle extracted from Sikhote-Alin iron meteorite. Adopted from [11].

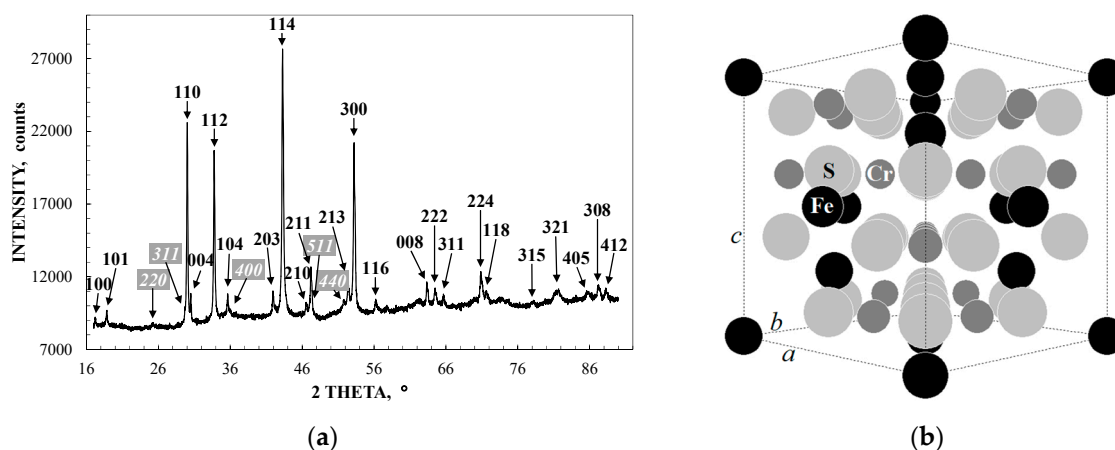


Figure 10. Characterization of troilite inclusion extracted from Sikhote-Alin iron meteorite: (a) X-ray diffraction pattern with Miller indices for troilite reflections (in bold) and for daubréelite reflections (in bold italic); and (b) the unit cell structure of daubréelite found in troilite inclusion extracted from Sikhote-Alin iron meteorite; a , b , and c are the unit cell parameters; ●—Fe, ●—Cr, and ●—S. Adopted from [11].

Magnetization measurements of the troilite inclusion extracted from the Sikhote-Alin iron meteorite demonstrated two features in the ZFC/FC curves (Figure 11a): (i) a distinguished peak at 74 K; and (ii) a sharp magnetic transition at 168 K. It is well known that daubréelite has the ferrimagnetic–paramagnetic phase transition around 177 K (see, for instance, [30] and references therein) while recently a transition temperature of 166.5 K was found in [31]. Therefore, the magnetic phase transition at 168 K can be assigned to the ferrimagnetic–paramagnetic phase transition in daubréelite in the troilite inclusion. Based on the data about the cubic to triclinic phase transition in daubréelite at ~60 K [32], the peak around 74 K can be assigned also to another phase transition in daubréelite found in the troilite inclusion. Similar magnetization behavior was observed earlier for troilite extracted from the Nantan iron meteorite, and phase transitions at 70 and 169 K were related to the phase transitions in daubréelite presented in troilite [33]. Therefore, both features in the ZFC/FC curves demonstrate the presence of daubréelite in the troilite inclusion extracted from the Sikhote-Alin iron meteorite.

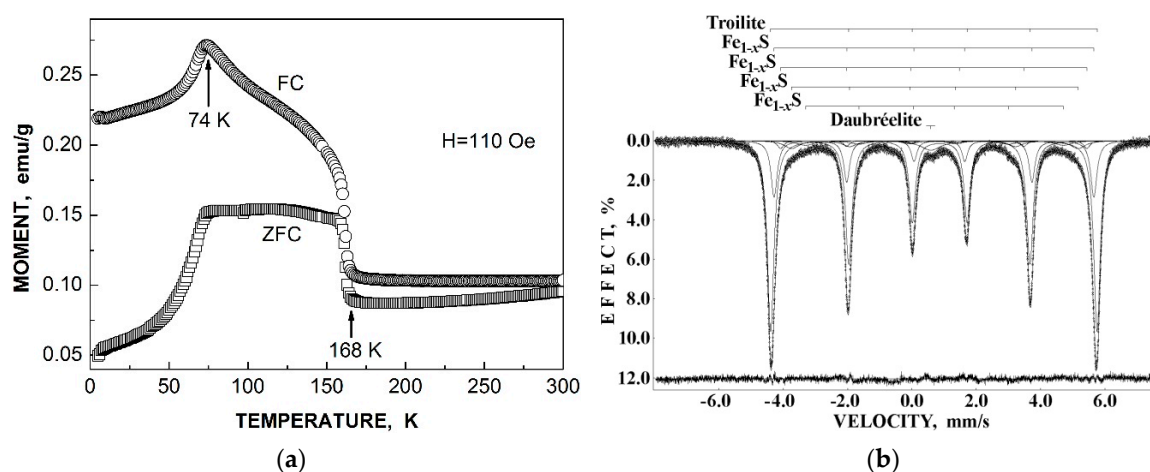


Figure 11. Troilite inclusion extracted from the Sikhote-Alin iron meteorite: (a) zero-field-cooled (ZFC) and field-cooled (FC) magnetization curves; and (b) Mössbauer spectrum measured at 295 K: indicated components are the result of the fit with a simulation of the full static Hamiltonian for the troilite component, the differential spectrum is shown below. Data adopted from [11].

The room temperature Mössbauer spectrum of the troilite inclusion extracted from the Sikhote-Alin iron meteorite is shown in Figure 11b. Originally, in [11], this spectrum was fitted using the full static Hamiltonian for troilite component. However, here we present a simple fit using a simulation of the full static Hamiltonian for troilite component and an additional four sextets for non-stoichiometric troilite Fe_{1-x}S for better observation of an additional spectral component related to daubréelite. Its spectral component has a single-peak shape with the following parameters: $\Gamma = 0.776 \pm 0.008$ mm/s, $\delta = 0.584 \pm 0.009$ mm/s, and $A = 2.6(3)$ %. This single peak disappears in the spectrum measured at 90 K [11] due to the magnetic phase transition and the appearance of a very small magnetic sextet related to daubréelite, extraction of which is very difficult in the spectrum with many overlapped sextets. It is well known that the Mössbauer spectra of daubréelite demonstrate a single peak component only above Curie temperature (see, for instance, [34]). The room temperature Mössbauer spectrum of the polycrystalline synthetic FeCr_2S_4 sample measured in [35] shows a single peak with $\delta = 1.2$ mm/s that is twice larger than those obtained for daubréelite found in the troilite inclusion extracted from the Sikhote-Alin iron meteorite. However, other results obtained earlier in [36,37] demonstrate similar δ values: ~ 0.59 mm/s.

3.4. Magnesioferrite in the Fusion Crust of Chelyabinsk LL5 Fragment

The fusion crust is a glass-like solidified melt resulting from meteorite surface combustion in the Earth's atmosphere during its fall. Various studies of meteorite fusion crusts showed formation of magnetite Fe_3O_4 , a spinel resulting from iron oxidation during combustion of the Fe-Ni-Co alloy [38,39]. We studied the fusion crust removed from ordinary chondrite Chelyabinsk LL5 fragment No 1a [10]. The XRD pattern of the fusion crust from Chelyabinsk LL5 fragment No 1a is shown in Figure 12a. The fit of this pattern using the Rietveld full profile analysis demonstrated the presence of olivine (~ 50 wt. %), pyroxene (~ 27 wt. %) and troilite (~ 4 wt. %) phases, Fe-Ni-Co alloy (~ 1 wt. %) and an additional phase related to magnesioferrite (~ 18 wt. %) instead of magnetite. The two main reflexes $[2\ 2\ 0]$ and $[3\ 1\ 1]$ at $2\Theta \sim 30^\circ$ and $\sim 35.5^\circ$, respectively, corresponding to magnesioferrite (PDF 01-089-6188), are clearly seen in the X-ray diffractogram, confirming the presence of magnesioferrite. There is an X-ray amorphous halo in 2Θ range $\sim 30\text{--}36^\circ$ that may be a result of the presence of some amount of nanosized magnesioferrite particles in the glass-like fusion crust. The first Mössbauer spectrum of the fusion crust from Chelyabinsk LL5 fragment No 1a, which should only be considered as a preliminary result, is shown in Figure 12b. In this spectrum, a pronounced six-line pattern with larger hyperfine field than that for sextets related to the Fe-Ni-Co alloy and troilite is clearly seen. The best fit of this spectrum revealed five magnetic sextets and five quadrupole doublets, as shown in Figure 12b. Besides two sextets related to Fe-Ni-Co alloy and troilite, respectively, and four quadrupole doublets related to the M1 and M2 sites in both olivine and pyroxene, three additional magnetic sextets with the following parameters were found: (1) $\delta = 0.271 \pm 0.020$ mm/s, $H_{\text{eff}} = 481.0 \pm 0.6$ kOe, $A = \sim 16(2)$ %; (2) $\delta = 0.528 \pm 0.029$ mm/s, $H_{\text{eff}} = 479.0 \pm 1.3$ kOe, $A = \sim 6(1)$ %; and (3) $\delta = 0.562 \pm 0.020$ mm/s, $H_{\text{eff}} = 444.6 \pm 1.8$ kOe, $A = \sim 11(1)$ %. One additional quadrupole doublet with parameters $\delta = 0.502 \pm 0.026$ mm/s, $\Delta E_Q = 0.993 \pm 0.047$ mm/s, and $A = \sim 7(1)$ % was found.

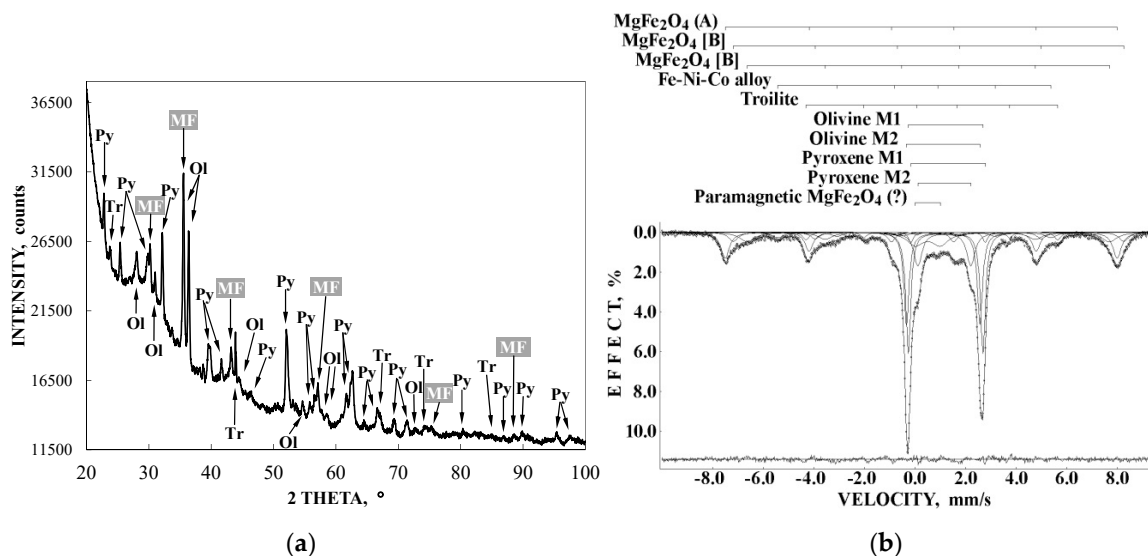


Figure 12. The fusion crust from Chelyabinsk LL5 fragment 1a: (a) X-ray diffraction pattern, arrows indicate reflexes of the main phases such as Ol (olivine), Py (pyroxene), Tr (troilite), and MF (magnesioferrite); and (b) Mössbauer spectrum measured at 295 K: indicated components are the result of the preliminary fit, the differential spectrum is shown below. Adopted from [10].

It is well known that magnesioferrite has a spinel structure with Fe^{3+} and Mg^{2+} cations in both tetrahedral (A) and octahedral [B] positions in different proportions within the formula: $(\text{Mg}_{1-x}\text{Fe}_x)_\text{A}[\text{Mg}_y\text{Fe}_{2-y}]_\text{B}\text{O}_4$. Mössbauer spectra of the bulk magnesioferrite usually demonstrate two magnetic sextets related to the ^{57}Fe in both (A) and [B] positions, as shown above in Section 3.1 (see [28,29]). Mössbauer hyperfine parameters permit sextets related to two different positions in spinel to be distinguished, because the values of δ are smaller with larger values of H_{eff} for sextets related to (A) positions while δ values are larger with smaller values of H_{eff} for sextets related to [B] positions. However, in the case of nanosized magnesioferrite the Mössbauer spectra were fitted using three magnetic sextets: one sextet was related to (A) positions while two sextets were related to [B] positions, as well as one quadrupole doublet related to the paramagnetic state of the smallest magnesioferrite particles [40]. Moreover, the values of $\delta = 0.37$ mm/s and $\Delta E_Q = 0.99$ mm/s obtained for the paramagnetic quadrupole doublet in [40] appeared to be close to above-mentioned Mössbauer parameters for a paramagnetic doublet revealed in the spectrum of the fusion crust in [10]. Therefore, sextet (1) was related to the ^{57}Fe in (A) positions while sextets (2) and (3) were assigned to the ^{57}Fe in [B] positions. The rest quadrupole doublet can be associated with nanosized magnesioferrite particles which are in the paramagnetic state. Thus, the first study of the fusion crust from Chelyabinsk LL5 fragment No 1a using XRD and Mössbauer spectroscopy observed the presence of magnesioferrite instead of magnetite.

4. Conclusions

Different meteorites (stony, stony-iron and iron) contain the minor spinel phases as accessories to the main minerals. Therefore, observation of the iron-bearing spinels in the Mössbauer spectra of bulk meteorite materials is not easy. Nevertheless, application of the high velocity resolution Mössbauer spectroscopy permits us to observe the minor spectral components in the complex meteorite spectra related to spinel phases. The complex study, using optical microscopy, scanning electron microscopy with energy dispersive spectroscopy, X-ray diffraction and magnetization measurements, in addition to Mössbauer spectroscopy, permits us to identify and prove the presence of iron-bearing spinels in meteorites. Thus, it is possible to observe various spinels such as chromite, hercynite, magnesiochromite, daubréelite and magnesioferrite in different meteorites using Mössbauer spectroscopy.

Author Contributions: Conceptualization, M.I.O.; reviewed measurements were carried out mainly by: A.A.M. (optical microscopy), A.A.M., M.I.O. (SEM with EDS), A.V.C. (XRD, full profile Rietveld analysis), I.F. (magnetization measurements and analysis), A.A.M., M.I.O. (Mössbauer measurements and spectra fits); writing—original draft preparation, M.I.O.; writing—review and editing, A.A.M., I.F., A.V.C.

Acknowledgments: The authors wish to thank all their colleagues in various studies, reviewed in the present work, for fruitful cooperation: Dr. V.I. Grokhovsky, Dr. V.A. Semionkin, Dr. E.V. Petrova, Dr. M.Yu Larionov, Dr. M.S. Karabanalov, M.V. Goryunov and G.A. Yakovlev (Ural Federal University, Ekaterinburg); Prof. E. Kuzmann, Prof. Z. Homonnay and Z. Bendő (Eötvös Loránd University, Budapest); Dr. Z. Klencsár (Centre for Energy Research, Hungarian Academy of Sciences, Budapest); and Dr. T. Kohout (University of Helsinki, Helsinki). This work was supported by the Ministry of Science and Higher Education of the Russian Federation (the Project No. 3.1959.2017/4.6) and by Act 211 of the Government of the Russian Federation, contract No. 02.A03.21.0006.

Conflicts of Interest: The authors declare no conflict of interest.

References

1. Weisberg, M.K.; McCoy, T.J.; Krot, A.N. Systematics and evaluation of meteorite classification. In *Meteorites and the Early Solar System II*; Lauretta, D.S., McSween, H.Y., Jr., Binzel, R.P., Eds.; University of Arizona Press: Tucson, AZ, USA, 2006; pp. 19–52. ISBN 9780816525621.
2. Jarosewich, E. Chemical analysis of meteorites: A compilation of stony and iron meteorites analyses. *Meteoritics* **1990**, *25*, 323–337. [[CrossRef](#)]
3. Rubin, A.E. Mineralogy of meteorite groups. *Meteorit. Planet. Sci.* **1997**, *32*, 231–247. [[CrossRef](#)]
4. Sprenkel-Segel, E.L.; Hanna, S.S. Mössbauer analysis of iron in stone meteorites. *Geochim. Cosmochim. Acta* **1964**, *28*, 1913–1931. [[CrossRef](#)]
5. Dos Santos, E.; Gattacceca, J.; Rochette, P.; Scorzelli, R.B.; Fillion, G. Magnetic hysteresis properties and ^{57}Fe Mössbauer spectroscopy of iron and stony-iron meteorites: Implications for mineralogy and thermal history. *Phys. Earth Planet. Inter.* **2015**, *242*, 50–64. [[CrossRef](#)]
6. Sato, W.; Nakagawa, M.; Shirai, N.; Ebihara, M. Mössbauer spectroscopic study on the composition of Fe-containing minerals in ordinary chondrites, Miller Range 07710 and Yamato 790272. *Hyperfine Interact.* **2018**, *239*. [[CrossRef](#)]
7. Oshtrakh, M.I.; Grokhovsky, V.I.; Petrova, E.V.; Larionov, M.Y.; Goryunov, M.V.; Semionkin, V.A. Mössbauer spectroscopy with a high velocity resolution applied for the study of meteoritic iron-bearing minerals. *J. Mol. Struct.* **2013**, *1044*, 268–278. [[CrossRef](#)]
8. Oshtrakh, M.I.; Maksimova, A.A.; Goryunov, M.V.; Yakovlev, G.A.; Petrova, E.V.; Larionov, M.Y.; Grokhovsky, V.I.; Semionkin, V.A. Mössbauer spectroscopy with a high velocity resolution: Advances in the study of meteoritic iron-bearing minerals. In *Proceedings of the Workshop on The Modern Analytical Methods Applied to Earth and Planetary Sciences*; Gucsik, A., Ed.; The MicroMatLab Kft Hungary: Sopron, Hungary, 2015; pp. 43–86. ISBN 978-963-12-1410-9.
9. Maksimova, A.A.; Chukin, A.V.; Oshtrakh, M.I. Revealing of the minor iron-bearing phases in the Mössbauer spectra of Chelyabinsk LL5 ordinary chondrite fragment. In *Mössbauer Spectroscopy in Materials Science 2016, Proceedings of the International Conference of American Institute of Physics*; Tuček, J., Miglierini, M., Eds.; AIP Conference Proceedings; AIP Publishing: Melville, NY, USA, 2016; Volume 1781, p. 020016. [[CrossRef](#)]
10. Maksimova, A.A.; Oshtrakh, M.I.; Petrova, E.V.; Grokhovsky, V.I.; Semionkin, V.A. Study of Chelyabinsk LL5 meteorite fragment with light lithology and its fusion crust using Mössbauer spectroscopy with a high velocity resolution. In *Mössbauer Spectroscopy in Materials Science 2014, Proceedings of the International Conference of American Institute of Physics*; Tuček, J., Miglierini, M., Eds.; AIP Conference Proceedings; AIP Publishing: Melville, NY, USA, 2014; Volume 1622, pp. 24–29. [[CrossRef](#)]
11. Oshtrakh, M.I.; Klencsár, Z.; Petrova, E.V.; Grokhovsky, V.I.; Chukin, A.V.; Shtoltz, A.K.; Maksimova, A.A.; Felner, I.; Kuzmann, E.; Homonnay, Z.; et al. Iron sulfide (troilite) inclusion extracted from Sikhote-Alin iron meteorite: Composition, structure and magnetic properties. *Mat. Chem. Phys.* **2016**, *174*, 100–111. [[CrossRef](#)]
12. Kohout, T.; Haloda, J.; Halodová, P.; Meier, M.M.M.; Maden, C.; Busemann, H.; Laubenstein, M.; Caffee, M.W.; Welten, K.C.; Hopp, J.; et al. Annama H chondrite-mineralogy, physical properties, cosmic ray exposure, and parent body history. *Meteorit. Planet. Sci.* **2017**, *52*, 1525–1541. [[CrossRef](#)]

13. Maksimova, A.A.; Oshtrakh, M.I.; Chukin, A.V.; Felner, I.; Yakovlev, G.A.; Semionkin, V.A. Characterization of Northwest Africa 6286 and 7857 ordinary chondrites using X-ray diffraction, magnetization measurements and Mössbauer spectroscopy. *Spectrochim. Acta Part A Molec. Biomolec. Spectrosc.* **2018**, *192*, 275–284. [[CrossRef](#)]
14. Maksimova, A.A.; Kamalov, R.V.; Chukin, A.V.; Felner, I.; Oshtrakh, M.I. An analysis of orthopyroxene from Tsarev L5 meteorite using X-ray diffraction, magnetization measurement and Mössbauer spectroscopy. *J. Mol. Struct.* **2018**, *1174*, 6–11. [[CrossRef](#)]
15. Oshtrakh, M.I.; Maksimova, A.A.; Goryunov, M.V.; Petrova, E.V.; Felner, I.; Chukin, A.V.; Grokhovsky, V.I. Study of metallic Fe-Ni-Co alloy and stony part isolated from Seymchan meteorite using X-ray diffraction, magnetization measurement and Mössbauer spectroscopy. *J. Mol. Struct.* **2018**, *1174*, 112–121. [[CrossRef](#)]
16. Oshtrakh, M.I.; Semionkin, V.A. Mössbauer Spectroscopy with a high velocity resolution: Advances in biomedical, pharmaceutical, cosmochemical and nanotechnological research. *Spectrochim. Acta Part A Molec. Biomolec. Spectrosc.* **2013**, *100*, 78–87. [[CrossRef](#)] [[PubMed](#)]
17. Oshtrakh, M.I.; Semionkin, V.A. Mössbauer Spectroscopy with a high velocity resolution: Principles and applications. In *Mössbauer Spectroscopy in Materials Science 2016, Proceedings of the International Conference of American Institute of Physics*; Tuček, J., Miglierini, M., Eds.; AIP Conference Proceedings; AIP Publishing: Melville, NY, USA, 2016; Volume 1781, p. 020019. [[CrossRef](#)]
18. Maksimova, A.A.; Klencsár, Z.; Oshtrakh, M.I.; Petrova, E.V.; Grokhovsky, V.I.; Kuzmann, E.; Homonnay, Z.; Semionkin, V.A. Mössbauer parameters of ordinary chondrites influenced by the fit accuracy of the troilite component: An example of Chelyabinsk LL5 meteorite. *Hyperfine Interact.* **2016**, *237*, 33. [[CrossRef](#)]
19. Maksimova, A.A.; Oshtrakh, M.I.; Petrova, E.V.; Grokhovsky, V.I.; Semionkin, V.A. Comparison of iron-bearing minerals in ordinary chondrites from H, L and LL groups using Mössbauer spectroscopy with a high velocity resolution. *Spectrochim. Acta Part A Molec. Biomolec. Spectrosc.* **2017**, *172*, 65–76. [[CrossRef](#)] [[PubMed](#)]
20. Gattacceca, J.; Rochette, P.; Lagroix, F.; Mathé, P.E.; Zanda, B. Low temperature magnetic transition of chromite in ordinary chondrites. *Geophys. Res. Lett.* **2011**, *38*, L10203. [[CrossRef](#)]
21. Maksimova, A.A.; Oshtrakh, M.I.; Grokhovsky, V.I.; Petrova, E.V.; Semionkin, V.A. Mössbauer spectroscopy of H, L and LL ordinary chondrites. *Hyperfine Interact.* **2016**, *237*, 134. [[CrossRef](#)]
22. Dézsi, I.; Szűcs, I.; Sváb, E. Mössbauer spectroscopy of spinels. *J. Radioanal. Nucl. Chem.* **2000**, *246*, 15–19. [[CrossRef](#)]
23. Lenaz, D.; Skogby, H.; Princivalle, F.; Hälenius, U. Structural changes and valence states in the MgCr₂O₄–FeCr₂O₄ solid solution series. *Phys. Chem. Mineral.* **2004**, *31*, 633–642. [[CrossRef](#)]
24. Osborne, M.D.; Fleet, M.E.; Bancroft, G.M. Fe²⁺–Fe³⁺ ordering in chromite and Cr-bearing spinels. *Contrib. Mineral. Petrol.* **1981**, *77*, 251–255. [[CrossRef](#)]
25. Schmidbauer, E. ⁵⁷Fe Mössbauer spectroscopy and magnetization of cation-deficient Fe₂TiO₄ and FeCr₂O₄. Part I: ⁵⁷Fe Mössbauer spectroscopy. *Phys. Chem. Mineral.* **1987**, *14*, 533–641.
26. Quintiliani, M.; Andreozzi, G.B.; Skogby, H. Synthesis and Mössbauer characterization of Fe_{1+x}Cr_{2-x}O₄ (0 ≤ x < 2/3) spinel single crystals. *Period. Mineral.* **2011**, *80*, 39–55. [[CrossRef](#)]
27. Lenaz, D.; Skogby, H. Structural changes in the FeAl₂O₄–FeCr₂O₄ solid solution series and their consequences on natural Cr-bearing spinels. *Phys. Chem. Mineral.* **2013**, *40*, 587–595. [[CrossRef](#)]
28. De Grave, E.; Govaert, A.; Chambaere, D.; Robbrecht, G. A Mössbauer effect study of MgFe₂O₄. *Physica B+C* **1979**, *96*, 103–110. [[CrossRef](#)]
29. Lenaz, D.; Skogby, H.; Princivalle, F.; Hälenius, U. The MgCr₂O₄–MgFe₂O₄ solid solution series: Effects of octahedrally coordinated Fe³⁺ on T–O bond lengths. *Phys. Chem. Miner.* **2006**, *33*, 465–474. [[CrossRef](#)]
30. Park, J.Y.; Kim, K.J. Magnetotransport and magnetic properties of sulfospinel Zn_xFe_{1-x}Cr₂S₄. *Hyperfine Interact.* **2006**, *169*, 1267–1272. [[CrossRef](#)]
31. Dey, K.; Indra, A.; Giri, S. Critical behavior of multiferroic sulpho spinel compounds: MCr₂S₄ (M = Co & Fe). *J. Alloys Comp.* **2017**, *726*, 74–80. [[CrossRef](#)]
32. Mertinat, M.; Tsurkan, V.; Samusi, D.; Tidecks, R.; Haider, F. Low-temperature structural transition in FeCr₂S₄. *Phys. Rev. B* **2005**, *71*, 100408(R). [[CrossRef](#)]

33. Čuda, J.; Kohout, T.; Tuček, J.; Filip, J.; Medřík, I.; Mashlan, M.; Zbořil, R. Mössbauer study and magnetic measurement of troilite extract from Natan iron meteorite. In *Mössbauer Spectroscopy in Materials Science 2012, Proceedings of the International Conference of American Institute of Physics*; Tuček, J., Machala, L., Eds.; AIP Conference Proceedings; AIP Publishing: Melville, NY, USA, 2012; Volume 1489, pp. 145–153. [[CrossRef](#)]
34. Klencsár, Z.; Kuzmann, E.; Homonnay, Z.; Vertes, A.; Simopoulos, A.; Devlin, E.; Kallias, G. Interplay between magnetic order and the vibrational state of Fe in FeCr₂S₄. *J. Phys. Chem. Solids* **2003**, *64*, 325–331. [[CrossRef](#)]
35. Chen, Z.; Tan, S.; Yang, Z.; Zhang, Y. Evidence for a non-double-exchange mechanism in FeCr₂S₄. *Phys. Rev. B* **1999**, *59*, 11172–11174. [[CrossRef](#)]
36. Van Diepen, A.M.; Lotgering, F.K.; Olijhoek, J.F. Effect of small variations of the Fe/Cr ratio on the ⁵⁷Fe Mössbauer spectra of FeCr₂S₄. *J. Magn. Magn. Mater.* **1976**, *3*, 117–119. [[CrossRef](#)]
37. Riedel, E.; Karl, R. Mössbauer Studies of Thiospinels. III. The System FeCr₂S₄–Feln₂S₄. *J. Solid State Chem.* **1981**, *38*, 40–47. [[CrossRef](#)]
38. Genge, M.J.; Grady, M.M. The fusion crusts of stony meteorites: Implications for the atmospheric reprocessing of extraterrestrial materials. *Meteorit. Planet. Sci.* **1999**, *34*, 341–356. [[CrossRef](#)]
39. Thaisen, K.G.; Taylor, L.A. Meteorite fusion crust variability. *Meteorit. Planet. Sci.* **2009**, *44*, 871–878. [[CrossRef](#)]
40. Antic, B.; Jovic, N.; Pavlovic, M.B.; Kremenovic, A.; Manojlović, D.; Vucinic-Vasic, M.; Nikolić, A.S. Magnetization enhancement in nanostructured random type MgFe₂O₄ spinel prepared by soft mechanochemical route. *J. App. Phys.* **2010**, *107*, 043525. [[CrossRef](#)]



© 2019 by the authors. Licensee MDPI, Basel, Switzerland. This article is an open access article distributed under the terms and conditions of the Creative Commons Attribution (CC BY) license (<http://creativecommons.org/licenses/by/4.0/>).